International Journal of Environmental Sciences
ISSN: 2229-7359
Vol. 11 No. 3S, 2025
https://www.theaspd.com/ijes.php

Evaluation of Red Mud as an Adsorbent for Heavy Metal Removal from Industrial Wastewater in the Damonjodi Region, Odisha

Maruwada Srinivasan[1] ;Ramprasad Naik Desavathu[2] ,Rakesh Roshan Dash[3]

[1]Research Scholar, Dept. of Civil Engineering, GIET University, Gunupur, Odisha, India. Email: srinivasan.maruwada@giet.edu

[2] Professor, Dept. of Civil Engineering, GIET University, Gunupur, Odisha, India. Email: dnaik@giet.edu.

[3] Associate Professor, Dept. of Civil Engineering, VSSUT Burla, Sambalpur, Odisha, India, Email: rrdash@gmail.com

Abstract

A significant global issue involves environmental contamination, particularly by heavy metal ions found in wastewater. It is usual practice to tackle this problem using ion exchange, chemical precipitation, coagulation, membrane separation, reverse osmosis, and adsorption procedures. In order to purify wastewater of various heavy metal ions, especially those that have proved harmful to living things, a wide range of adsorbents have been produced. In this paper, investigates the effectiveness of Red Mud (RM) as an adsorbent for removing contaminants from industrial wastewater. RM, a byproduct of alumina production, was utilized due to its potential to adsorb heavy metals and other pollutants effectively. This research focused on optimizing various parameters such as pH, adsorbent dosage, contact time, and initial concentration of contaminants to enhance adsorption efficiency. Both Langmuir and Freundlich isotherm models were employed to analyze the adsorption equilibrium, showing favorable adsorption characteristics with high correlation coefficients. The study concludes that RM holds promise as a sustainable and cost-effective adsorbent for treating industrial wastewater, offering significant potential for environmental remediation efforts. The experimental findings demonstrate that RM achieved a maximum adsorption capacity (q_m) of 13.33 mg/g according to the Langmuir isotherm, and a Freundlich isotherm yielded a maximum value of n = 2.21 for red mud.

Keywords: Industrial Waste, Contaminants, Red Mud (RM), Adsorption, Langmuir isotherm and Freundlich isotherm

1. INTRODUCTION

Industries are major consumers of water. Globally, they use about 22% of the total water produced, with this figure rising to as much as 60% in high-income countries. Projections suggest that by 2050, water usage in manufacturing industries could increase by 400%[1]. Industrial wastewater refers to the aqueous waste that results from the utilization of water in many processes in industry, including cooling towers, boilers, purification, and more. This effluent may include a wide variety of pollutants, both suspended and dissolved[2]. The most common types of industrial wastewater come from several manufacturing sectors, including the chemical and petrochemical, paper and pulp, food processing, tannery, and other related industries[3]. Heavy metal concentrations, salinity, turbidity, temperature extremes, non-neutral pH, and high organic strengths (ranging from 1 to 200 g/L) are typical characteristics of these wastewaters[4]. Various industries' wastewater, including those dealing with leather production, food processing and preservation, textile processing, and petroleum refining, might include elevated levels of salt[5]. Industrial wastewater is difficult to categorize since its composition changes based on the chemicals employed in the upstream processes and the kind of treatment it has received.

Industrial wastewater should ideally be treated before being either disposed of properly or recycled for uses such as landscaping and household cleaning. However, many nations lack efficient regulatory frameworks backed by regulatory agencies, making regulatory management of industrial effluent a regional issue[6]. Untreated industrial effluents account for 70% of developing-world dumps, says UNESCO[7]. Water discharge and reuse regulations are becoming increasingly strict in many nations, making it difficult for businesses to fulfill their obligations[8,9].

The possible danger that Emerging Contaminants (ECs) pose to both human and environmental health has recently raised significant concerns among environmentalists and government authorities. Chemicals used on a regular basis by people, hormones or medications given to cattle, and pesticides or nanomaterials applied to plants (to enhance nutrient absorption) are the three primary EC sources yet discovered[10]. There are a number of entry points for them into the environment. For example, most wastewater treatment plants (WWTPs) do not have the capability to extract ECs from the wastewater that is processed by ordinary human-used goods. The next steps include releasing treated wastewater back into water sources or using wastewater sludge as soil fertilizer, respectively. Both processes retain ECs. Livestock ECs are assimilated into their dung, while plant ECs are applied topically to soil and then, when it rains, are leached out into surrounding water sources. Figure 1 illustrates the release of ECs into water from these three main sources.

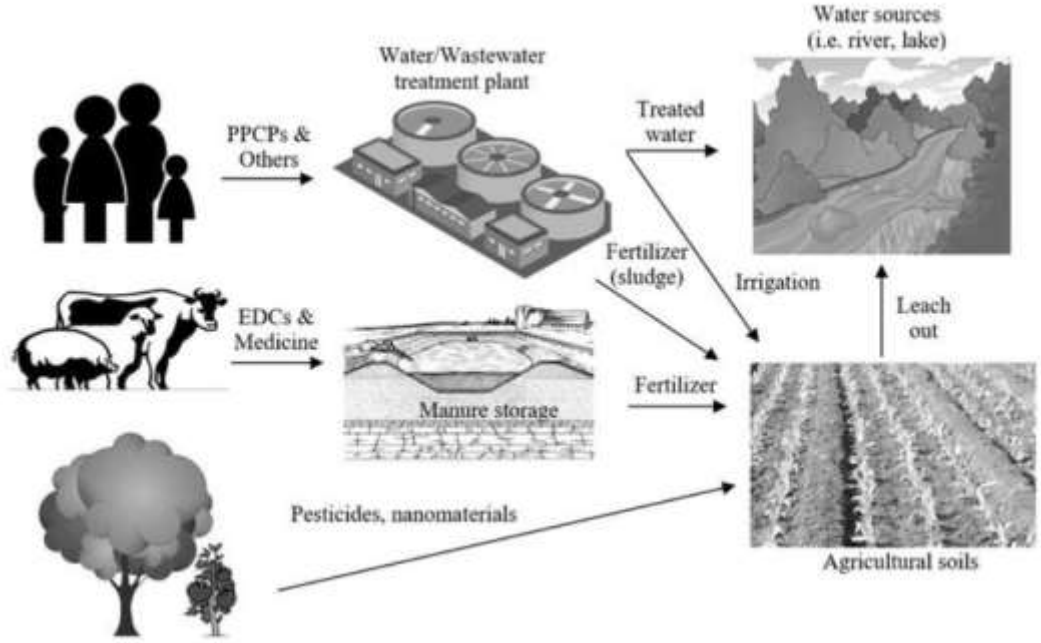

Figure 1: ECs into water sources and their origins[11].

Urbanization, industrialization, population expansion, and changes in agricultural and land use practices all contribute to an annual rise in water demand, especially potable water[12]. The accessibility of potable water is one of the world's most pressing issues, impacting billions of people. Sustainable water and wastewater management is essential to thriving communities, and governments and organizations throughout the globe have come to recognize this. Waters with poor elimination rates have been shown to contain several kinds of ECs, according to recent findings[13]. Additionally, there is a lack of data on the incidence, risk assessment, and ecotoxicological aspects of most ECs, making it impossible to forecast their aquatic environmental conditions[14]. This is partly due to the limitations of analytical methods in measuring low concentrations of ECs (typically at parts per billion or parts per trillion levels), the diversity of their chemical properties, and the complexity of the matrices involved[5].

1.1 Adsorption Process

Adsorption is a method of separation when an adsorbate is bound to an adsorbent surface in aqueous media through chemisorption, hydrogen bonding, van der Waals, or hydrophobic bonding[16]. A preferred method for removing organic contaminants from water sources is the adsorption procedure. Both the process's applicability and the success in achieving high levels of target parameters are affected by the physicochemical characteristics of the adsorbents used[17]. A simple operating system might make its implementation appealing for multiple systems when considering a low-cost adsorbent[18]. As a result of the formation of a covalent connection between the adsorbate and adsorbent, which is partially reversible, adsorption could be carried out using a wide variety of adsorbents[19].Figure 2 is a conceptual depiction of the adsorption process that shows the three components and how they interact with one other. In a ternary system, the driving force behind the adsorption mechanism is the attraction between the adsorbent and the adsorbate. There are a number of factors that contribute significantly to adsorption, including the affinities between the adsorbate and the solution, the adsorbent and the solution, and especially the hazardous components[20]. Phase transitions, such as those between liquids and solids, gases and liquids, or gas and solids, are the focus of adsorption, which involves the removal of components at these interfaces.

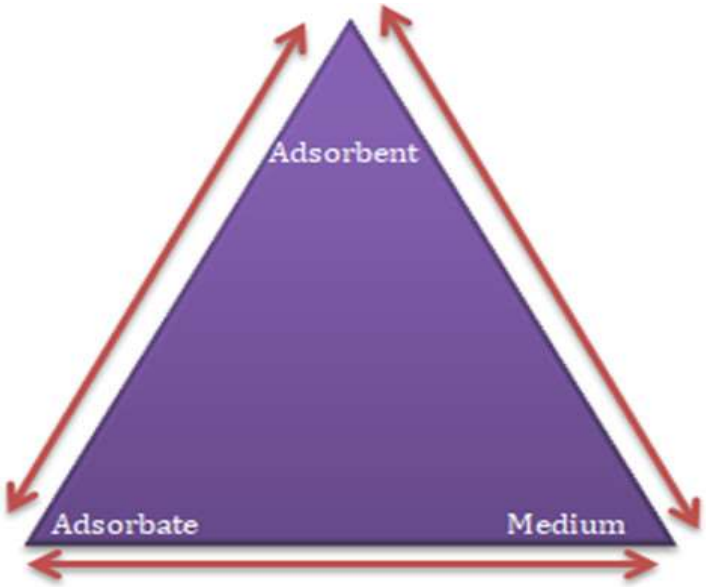

Figure 2: The interactions among the components in a ternary system[21].

2. REVIEW OF LITERATURE

Boskovic I. et al., (2024)[22]intended to investigate the feasibility of using geopolymers made of Red Mud (RM) and Fly Ash (FA) to filter out harmful contaminants like lead and copper ions from wastewater. Mixtures of RM and FA in varying proportions were produced by alkaline activation. They selected RMFAGP1, a geopolymer, for further study since it had the greatest compressive strength value of 29.54 MPa. The mineral composition and structure of RMFAGP1 were examined by physical-chemical characterization employing XRD, DRIFT, and SEM examination. They defined porosity and the particular surfaces needed for effective adsorption using BET analysis. To help with adsorption prediction, the batch equilibration technique was employed to get the PZC value. Acidity levels of 4 (88.5% adsorption efficiency) and 5 (99.4% adsorption efficiency) were shown to be optimal for copper and lead, respectively.

Le Q. et al., (2023)[23]looked at the combinations between lead and polypropylene (PP) using molecular dynamics modeling. When it comes to removing lead from water sources, PP is by far the most effective material. Lead removal from oil and petrochemical wastewater is of the utmost importance due to the prevalence of heavy metals in aquatic environments, including Pb,Cd, Hg, Cr, Zn, and Ni. This study's findings could come in handy when it comes time to remove lead from

wastewater treatment plants.

Chyad T. et al., (2023)[24]presented of this approach is to find affordable adsorbents for industrial wastewater treatment using pine cones as plant waste adsorbents. The batch method is utilized to determine the adsorbent dose and beginning concentration of the adsorbate. To find out how well it removed heavy metals and other contaminants (turbidity, TSS, and TDS), researchers utilized a pine cone plant waste sample. An adsorbent for the elimination of zinc ions from wastewater including industrial contaminants was activated carbon made from Turkish pine cones (ACPC). Activated carbon from pine cones was subjected to surface analysis to determine its particular surface area and distribution of pore sizes. Researchers looked at the best conditions, including pH, mixing speed, adsorbent dose, equilibrium time, and temperature. The equilibrium data were assessed utilizing models such as Freundlech, Elvich, and Langmuir isotherms. The Langmuir isotherm framework was the most appropriate for the equilibrium data.

An D. et al., (2023)[25]said that the approach, known as purifying wastewater using waste materials (PWWM), could reduce pollution while significantly increasing the secondary use of industrial waste materials. Despite this, PWWM has not yet seen widespread implementation due to its secondary use process's significant difficulty and poor organic pollutant purification performance. In this work, a recoverable adsorbent known as ZAS/GRM adsorbent is created by modifying waste Granular Red Mud (GRM) with Zinc Aluminum Silicate (ZAS). Heavy metal ions may efficiently solidify and restrict their outflow by using the ZAS, which demonstrates remarkable adsorption capability by securely anchoring onto the surface of GRM. Our CR purification results show that the ZAS/GRM adsorbent has a CR adsorption capacity of 3.509 mg g−1, which is four times more than pure GRM's 0.820 mg g−1. The PWWM technique is shown to be extremely successful, which might motivate more research on waste reuse.

Carvalheiras J. et al., (2023)[26]realized that RM and Metakaolin could be utilized as solid precursors to create geopolymer monoliths. These monoliths would have hierarchical porosity and an appropriate compressive strength of 4.5 MPa, making them ideal for usage as bulk-type sorbents rather than powdered ones. This innovative method, which utilizes hazardous trash to create solid structures that can treat wastewater including lead, is not only practical but also provides excellent results.The highest lead removal capacity of 30.7 mg/g achieved by the porous bodies (at pH 5, C0 = 600 ppm) was one of the more remarkable findings reported for bulk-type geopolymers. The monoliths could be used in several sorption cycles with the right desorption agent because they could be regenerated after sorption without drastically reducing their performance.

Xu W. et al., (2022)[27]explore the potential of RM-based geopolymer pervious concrete as an environmentally friendly method for AMD heavy metal removal. The rapid decrease of acid and removal of metals by the geopolymer are both caused by the dissolving of portlandite in RM. There seems to be a preponderance of metal hydroxide precipitation as a tool for metal removal. At an ideal environment with an influent pH of 4.0 and a hydraulic retention duration of 24 hours, RM-based geopolymer prior concrete was able to eliminate Cu(II), Mn(II), Cd(II), and Zn(II) to concentrations of up to 10 mg/L, 10 mg/L, 1.6 mg/L, and 16 mg/L, respectively. The consumption of OH^- is increased due to the hydrolysis of Fe(III) produced from RM when the influent pH is only 2.5. Additionally, CaSO4 precipitation enhances portlandite breakdown and metal removal at an influent pH of 4.0. Therefore, it is clear that RM could be used to make pervious concrete with geopolymers for AMD purification.

Lyu F. et al., (2021)[28]included a hydrothermal technique for RM modification using sodium hydroxide and colloidal silica under moderate circumstances; then used this modified mud to adsorb Pb(II) ions in water-based systems. The adsorption isotherm was well-fit by the Langmuir and Dubinin-Radushkevichframework, suggesting that the modified RM primarily used monolayer physical adsorption to remove lead ions from water. Validating its high efficiency adsorption ability, the fitting findings show that the modified RM has a saturation adsorption capacity of Pb (II) of 551.11 mg/g. The presence of $PbCO_3$ and $Pb_3(CO_3)_2(OH)_2$ was discovered by XRD, FTIR, XPS, and SEM-EDS. Some

have proposed that ion exchange and precipitation work together to explain the adsorption process.

Elboughdiri N. et al., (2020)[29]evaluated the efficacy of natural zeolites in eliminating heavy metals from industry effluent by studying their adsorption behaviour of $Cu2^{+}$, $Pb2^{+}$, and $Cd2^{+}$ from synthetic metal solutions. The findings indicate that the removal efficiency of $Cu2^{+}$ increased from 60% with 1 gram of adsorbent to 99% with 10 grams. Similarly, it increased from 62% at pH 1 to 94% at pH 7 of the initial solution. Agitation speed also played a role, with efficiency rising from 90% at 100 rpm to 94% at 300 rpm. Rising from an initial concentration of 100 mg/l at 0.5 mg/g to 400 mg/l at 2.1 mg/g, the adsorption capacity showed a significant rise. There was an initial burst of rapid adsorption for Cu2+, Pb2+, and Cd2+ ions, followed by a gradual decrease.

3. RESEARCH METHODOLOGY

3.1 Problem Statement

Industrial waste treatment using adsorption in Odisha'sDamonjodi area and the efficacy of the technologies used. As a result of the pollution that has leaked into nearby water sources, this region is experiencing environmental problems. This study's primary goal is to better understand industrial effluents by cataloguing the different contaminants, their amounts, and the adsorption materials and techniques that have been evaluated. Research in this area aims to improve water quality and ecosystem health in the Damonjodi region by lowering the environmental impact of industrial waste. It does this by comparing the adsorption capacity and efficiency of various adsorbents in order to provide sustainable and cost-effective solutions.

3.2 Techniques Used

In this section we have used the two approaches i.e., X-Ray Diffraction (XRD) and Scanning Electron Microscopy (SEM) to removing contaminants from industrial waste.

3.2.1 XRD

XRD remains a very effective and adaptable method that is extensively used to comprehend the microstructure, phase composition, and structure of crystalline materials. After Max von Laue found that crystals scatter X-rays, revealing their structure in the resulting pattern, the method was created in the early 1900s[30]. These results provided further evidence for the space lattice theory and for the wave-particle duality of X-rays [31]. A crystalline substance's periodic atomic arrangement causes monochromatic X-rays to undergo both constructive and destructive interference when they contact with the material. The structural features of the sample could be inferred by capturing the diffraction pattern caused by the interference and using a detector. For many years after its discovery, XRD has been an indispensable tool for many scientific disciplines, including materials science, chemistry, biology, and physics. It has been essential in the search for, creation of, and improvement upon new compounds with uniquely suited characteristics for a wide range of real-world and theoretical uses[32].

William Henry Bragg and his son William Lawrence Bragg established Bragg's law, which is the basis of XRD[33]. It is possible to determine the circumstances for constructive interference of X-rays in a crystal lattice using the given equation, which depends on Bragg's law:

$$n.\lambda = 2.d\ Sin\theta \quad (1)$$

- n represents the order of the diffraction peak, typically set to 1 for primary peaks.
- Where λ represents the incident X-rays' wavelength.
- The separation between the crystal planes, denoted as d;
- θ refers to the angle that exists between the crystal plane and the incoming X-rays [34].

3.2.2 SEM

SEM is an essential tool for inspection in the semiconductor industry [35,36]. In addition, the reviewers behind this piece want to use the microscope photos for future projects. Therefore, the focus of this

scoping review will be on SEM. While acoustic microscopy and Scanning Transmission Electron Microscopy (STEM) are the most common forms of microscopy used in inspection activities, other kinds of microscopies are also utilised. It is worth mentioning that the ML and DL approaches covered in this study could potentially extended to pictures captured by other types of microscopes or with other sorts of flaws in addition to SEM images. While scanning electron microscopy (SEM) is the gold standard in semiconductor production, alternative microscopy techniques could be just as effective in certain situations. The properties of the so-called location of principal excitation are defined by the beam electron energy and the specimen's atomic number. While increasing the energy results in longer penetration lengths, it also reduces the surface resolution. Because it becomes simpler to block the penetration of electrons as the number of particles increases, a lesser depth is produced by an increase in atomic number. Therefore, to determine the optimal beam energy, it is important to find a middle ground and evaluate the circumstances. Figure 3 shows a simplified design of a SEM with all of its individual parts.

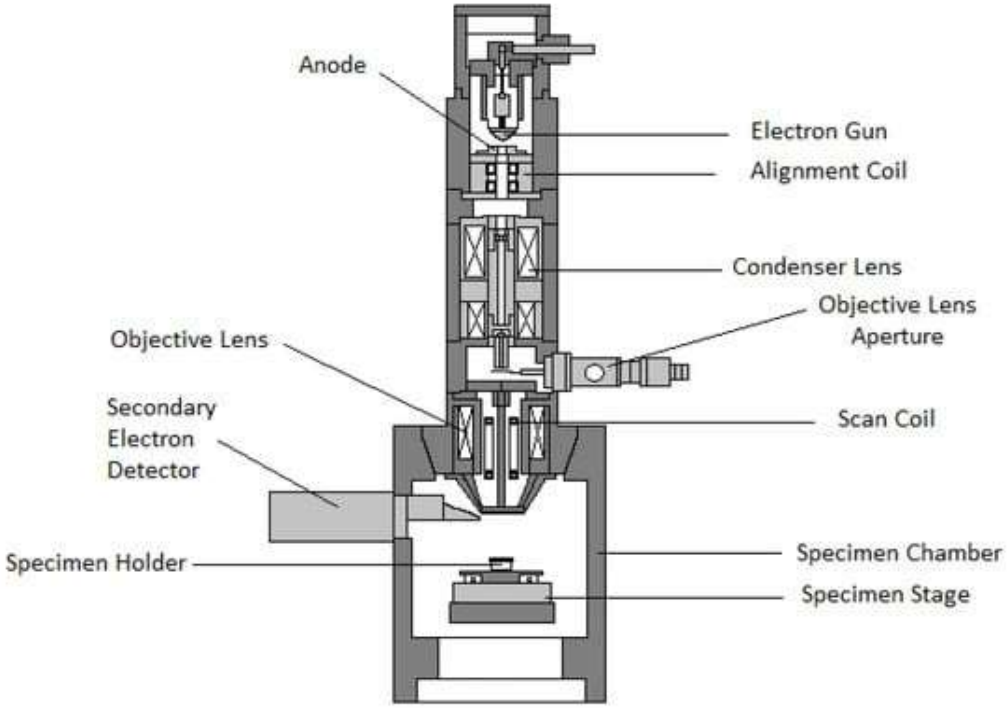

Figure 3: Architecture of SEM[37]

3.3 MATERIAL AND METHODS

3.3.1 Data Collection

Damonjodi, Odisha, India's NALCO was the source of the RM as shown in Figure 4. The process of making alumina (aluminium oxide) from bauxite produces it as a by-product. Typically, for every tonne of alumina produced, between 1.2 and 1.6 metric tonnes of RM is obtained. After a thorough washing with distilled water, the RM was heated in a furnace for eight hours at 110 °C. The next step was to let it cool to room temperature, pound it into a powder, then filter it through -44 and +52 determination sieves. For the batch trials, the strained material was then dried in a desiccator.

Figure 4: Nalco Red Mud disposal pond, Damanjodi, Odisha

Nalco's RM is disposed of as a slurry with 40% solid content by volume, transported via pipeline as illustrated in Figure 5. Over time, the water in the RM settles, causing the mud to dry. The settled liquid is recycled back into the aluminum refinery for various purposes, while the solid component (RM) remains unused. During the drying process, unstable $Ca(OH)_2$ surfaces and reacts with CO_2, forming stable calcium carbonate ($CaCO_3$). This stable $CaCO_3$ accumulates on the surface of the RM and can be dispersed as dust by the wind. To prevent the inclusion of stable $CaCO_3$ in the RM samples for this research, the top layer was removed before sample collection.

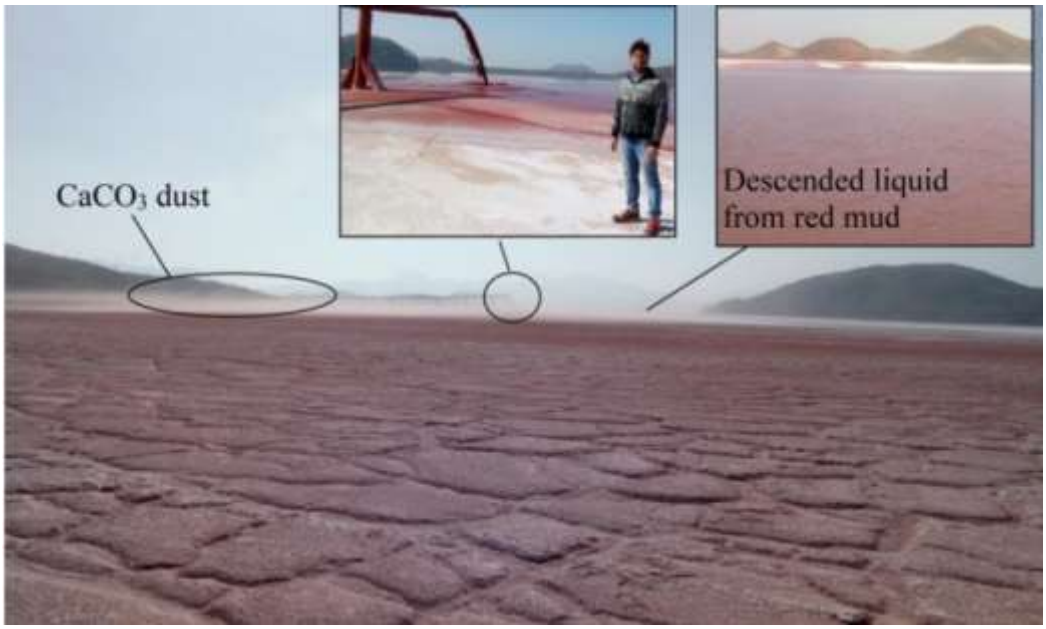

Figure 5: Slurry disposal of RM in NALCO, Damanjodi, Odisha

3.3.2 Characterization

The RM samples that were created were examined using a BET surface analyzer, a particle size analyzer, XRD, and a scanning electron microscope (SEM). The ASAP Micromeritics 2020 was used to estimate surface area by nitrogen desorption at a temperature of liquid nitrogen (−196°C). Degassing the samples at 200°C for 2 hours was done before analysis. To find the RM samples' surface areas, the BET equation was used. The XRD patterns were captured by means of a 40 kV and 30 mA Cu Kβ radiation-

equipped X'pert PRO, Pan Analytical Diffractometer. The scanning rate was 20 degrees per minute, and the scattering angles were 20 to 60 degrees. The RM samples were subjected to a particle size analysis utilising the Micromeritics Saturn DigiSizer II 5205. The data will be useful for calculating the surface area-related percentage of particles in various size groups.

The adsorbent samples were analyzed using a JSM IT-300 field emission SEM to determine their surface appearance and microstructure. At 15 kilovolts, this SEM could achieve a magnification of one million.They used a NETZS 402PC heat analyzer in a nitrogen environment to conduct thermogravimetric (TG) analyses on RM samples, with heating rates ranging from 30 to 1000∘C and a rate of 20∘C/min.Subsequent sections of the article address the findings from SEM and thermogravimetric analysis (TGA) that point to the presence of acid or heat-induced phase transitions.

30°C ± 1°C capped conical flasks containing 20 mL of phosphate solutions ranging from 50 mg/L to 1000 mg/L (made from KH2PO4) and 0.1 g of adsorbent were subjected to stirring for 8 hours in order to conduct the adsorption studies. After the solutions' equilibrium, the pulp filtering technique was used to filter them, and the phosphate content was determined utilizing the modified single solution approach, as outlined by Murphy and Riley [38] and the State Environmental Protection Administration [39].For the purpose of creating a calibration curve, a Shimadzu UV-1800 spectrophotometer was used to determine the absorbance at a wavelength of 882 nm for phosphate concentrations ranging from 0.02 to 0.2 mg of $PO4^{2-}$/L.This curve served as the foundation for determining the concentration of the unknown material. This was employed to ascertain the amount of phosphate that was absorbed per mass of adsorbent:

$$X = \frac{(C_i - C_f) * V}{m} \quad (2)$$

Ci and Cf are the starting and final concentrations of phosphate in mg/L, respectively, while Y denotes the concentration of adsorbed phosphate. A conical flask is used to agitate the solution, and the volume in liters is represented by V. The weight of the adsorbent is denoted by m. The Freundlich and Langmuir isotherms, which show the solute's equilibrium adsorption from a solution at a constant temperature, were used to measure the phosphate adsorption procedure on RM. That monolayer sorption happens at homogeneous, discrete places is one of the underlying assumptions of the Langmuir isotherm. One way to represent the Langmuir isotherm is:

$$X = \frac{kX_m C_{eq}}{1 + kC_{eq}} \quad (3)$$

In this context, X represents the amount of solute adsorbed, measured in mg of PO_4^{2-} per gram of adsorbent. C_{eq}denotes the equilibrium concentration of the solution in mg of PO_4^{2-} per liter.The monolayer adsorption capacity, denoted as X_m and given in mg/g, is proportional to a constant k that is associated with the free energy of adsorption. As a mathematical description of adsorption on heterogeneous surfaces, the Freundlich adsorption isotherm could be represented as:

$$QC = KC_{eq}^{1/m} \quad (4)$$

The relationship between concentration and the amount of adsorption under the empirical circumstances is stated in [40], and the constants K and n denote this nonlinearity.

3.3.3 Preparation of Synthetic Stock Solution

- **Preparation of Synthetic Lead Solution**

Using 1000 mL of deionized water to dissolve 1.598 g of lead nitrate, the concentration was set to 1000 mg/L. To get the right concentrations, this stock solution was diluted. A Pb(II) solution with a concentration of 50 mg/L was made from the stock solution and used for the adsorption procedure in this experiment.

- **Preparation of Synthetic Chromium Solution**

In 1000 mL of deionized water, 2.82 g of $K_2Cr_2O_7$ was dispersed to create a 1000 mg/L Cr(VI) stock

solution. Afterwards, more deionized water was added to this stock solution until it reached the required concentration of Cr(VI) of 50 mg/L.

3.3.4 Isotherms Modelling

Adsorption isotherm modellingdepict the adsorbent's interaction with the adsorbate and help to comprehend the adsorption process. Findings about surface characteristics and adsorption capacity are presented using the isotherm models. The Freundlich and Langmuir isotherm frameworks were used to comprehend the heavy metal ion adsorption procedures onto low-cost adsorbents.

- **Langmuir Isotherm**

According to the this model, where no connections between adsorbates on neighboring sites take place, metal ion adsorption happens by monolayer adsorption on a homogenous surface [41]. Common representations of the Langmuir equation include:

$$q_e = \frac{q_m K_L C_e}{1+K_L C_e} \tag{5}$$

Here is the equation expressed in its linear form:

$$\frac{1}{q_e} = \frac{1}{q_m} + \left(\frac{1}{q_m K_L}\right)\left(\frac{1}{C_e}\right) \tag{6}$$

Here, q_e stands for the maximum adsorption capacity, C_e for the equilibrium concentration of metal ions in the solution, K_L for the Langmuir constant, and mg/g for the quantity of metal ions adsorbed per unit mass of the adsorbent.

- **Freundlich isotherm**

Adsorption of metal ions onto a heterogeneous surface and subsequent molecular contacts are the underlying assumptions of the Freundlich isotherm model [42]. It is possible to express the Freundlich model as follows:

$$q_e = K_F C_e^{1/n} \tag{7}$$

The equation in its linear form can be expressed as:

$$log q_e = log K_F + \frac{1}{n} log\ C_e \tag{8}$$

Here, q_e is the volume of metal ions adsorbed per gramme of adsorbent (in milligrams/g), and C_e is the concentration of metal ions in solution at equilibrium (in milligrams/liter). The Freundlich adsorption isotherm calls for a constant n and a Freundlich constantK_F (mg/g) (mg/L). Important parameters include the R^2 value for linear regression; a value closer to 1 shows the best-fitting model [43].

Whereas C_e is the equilibrium concentration of metal ions in the solution (in milligrammes per litre), q_e is the quantity of metal ions adsorbed per gramme of adsorbent in this context. For the Freundlich adsorption isotherm, the parameters K_F (mg/g) (mg/L)n and n are important. One crucial parameter is the R^2 value for linear regression; a value closer to 1 show that the data is most suitable by the model.

4. RESULTS AND DISCUSSION

4.1Lead Pb (II) Ion Removal

4.1.1 Effect of pH

Initially, the aim of the batch adsorption tests was to determine how the adsorbent's absorption of Pb (II) ions was affected by the pH.Removing Pb (II) ions at various pH values was the goal of this study. The ion concentration was maintained at 50 mg/L and 0.5 g of adsorbent was given to each of the three agents. The pH values ranged from 1 to 10. The pH levels were measured using a digital meter manufactured by Hanna Instruments, and HCl and NaOH drops were used for pH changes.

At lower pH values (1-2), the concentration of H^+ ions was high, competing with lead ions for

adsorption sites and thereby reducing Pb (II) ion adsorption onto the adsorbents. Conversely, at higher pH values (8-10), elevated OH- ion concentrations resulted in the precipitation of lead hydroxide, leading to a decrease in adsorption efficiency. Figure 6 is a graph showing the correlation between pH and the proportion of Pb (II) ions removed. It was seen from the graph that RM attained its maximum adsorption at pH 5, resulting in a clearance percentage of 79.64%.

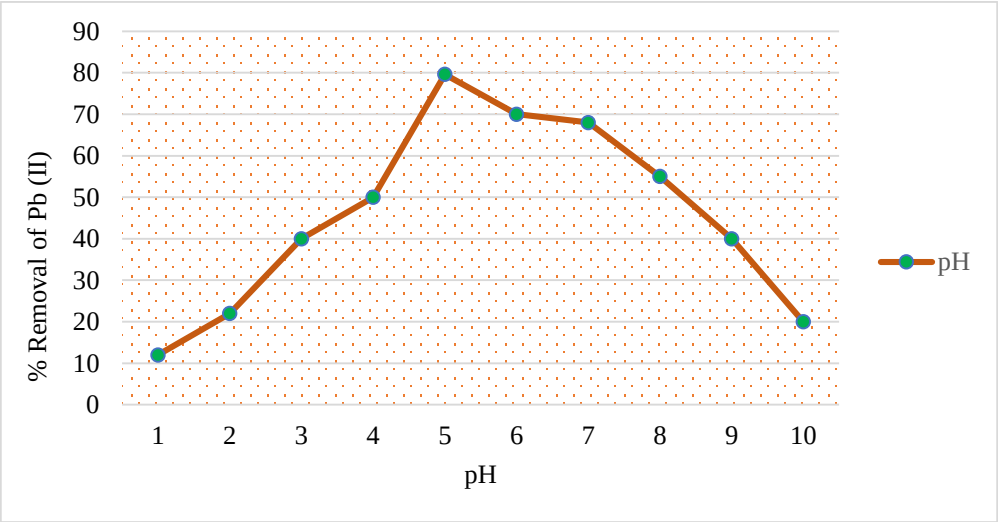

Figure 6: Changes in Pb (II) ion adsorption as a function of pH

4.1.2 Effect of absorbent dosage

Figure 7 presents the dosage of adsorbent plays a crucial role in managing the capital costs associated with adsorption. The primary focus of these investigations was the adsorption capacities of the adsorbents. The study assessed how varying dosages of adsorbent affected the percentage of lead (II) removed from a 50 mg/L aqueous solution. The dosages ranged from 0.1 g to 0.8 g. The experiments were conducted under optimal pH, time, and metal ion concentration conditions, which were kept constant throughout.The findings indicated that RM achieved maximum removal efficiency at 0.7 g of adsorbent, removing Pb (II) at a rate of 80.12%. This is because there are more active surface sites on the adsorbent, which makes them more available. Upon adding 0.7 g of adsorbent, removal efficiency reached equilibrium, showing no further improvement. Additional adsorbent beyond this point led to interactions with existing adsorption sites, causing aggregation of adsorbents and consequently slightly reducing their removal efficiency.

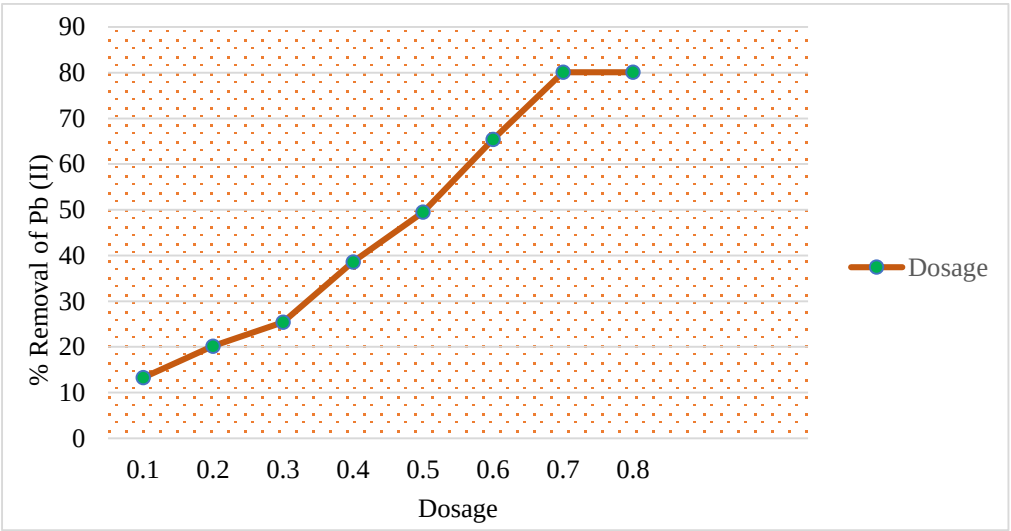

Figure 7:Relationship between adsorbent dosage and lead (II) ion adsorption

4.1.3 Effect of Contact Time

The operational cost is managed through contact time analysis, which was conducted in this experimental study. The impact of contact time was investigated using 50 mg/l of Pb (II) as an initial point, 0.7 g of optimized adsorbent, and a pH of 5. As shown in Figure 8, the concentration stayed the same even though the contact period ranged from fifteen to one hundred and three minutes.The figure demonstrates that the adsorbent's efficiency in removing Pb (II) was highest at the beginning of the adsorption process, when active sites were readily available and unoccupied. As time progressed, these sites became occupied by Pb (II) adsorbate, eventually reaching equilibrium. Figure 8 also indicates that the percentage removal of Pb (II) was initially rapid and high, stabilizing as contact time increased.The optimal contact time for Pb (II) removal using RM adsorbents was found to be 60 minutes, achieving a removal percentage of 79.12%.

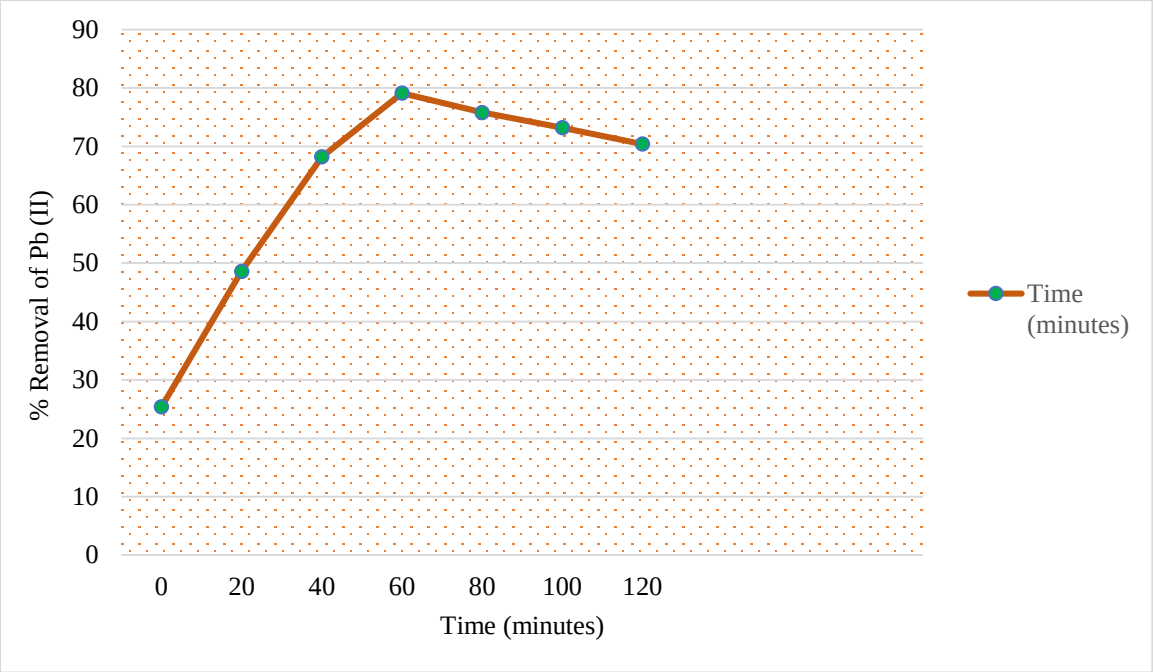

Figure 8: Variation in lead (II) ion adsorption with respect to contact duration

4.1.4 Effect of concentration of Pb (II) ions

They employed Pb (II) values between 50 and 100 mg/l to study the starting ion concentration treated with RM adsorbents. The experiments utilized the optimal pH, dosage, and time parameters to investigate the effectiveness of varying Pb (II) ion concentrations for removal. The established optimal adsorbent dose was tested against different ion concentrations.In Figure 9, the correlation between the percentage of Pb (II) ions removed and the beginning concentration is shown.Both adsorbents showed a high percentage of removal at low beginning concentrations (e.g., 50 mg/l) but a declining trend as ion concentrations grew (as shown in the image). Initial concentrations of 50 mg/l of Pb (II) were found to provide a clearance effectiveness of 79.64%. This decline in removal efficiency with increasing ion concentration can be attributed to the adsorbents initially having more available active sites when ion concentrations are lower, facilitating greater adsorption. As ion concentrations rise, available adsorbent sites become fewer, leading to decreased adsorption efficiency.

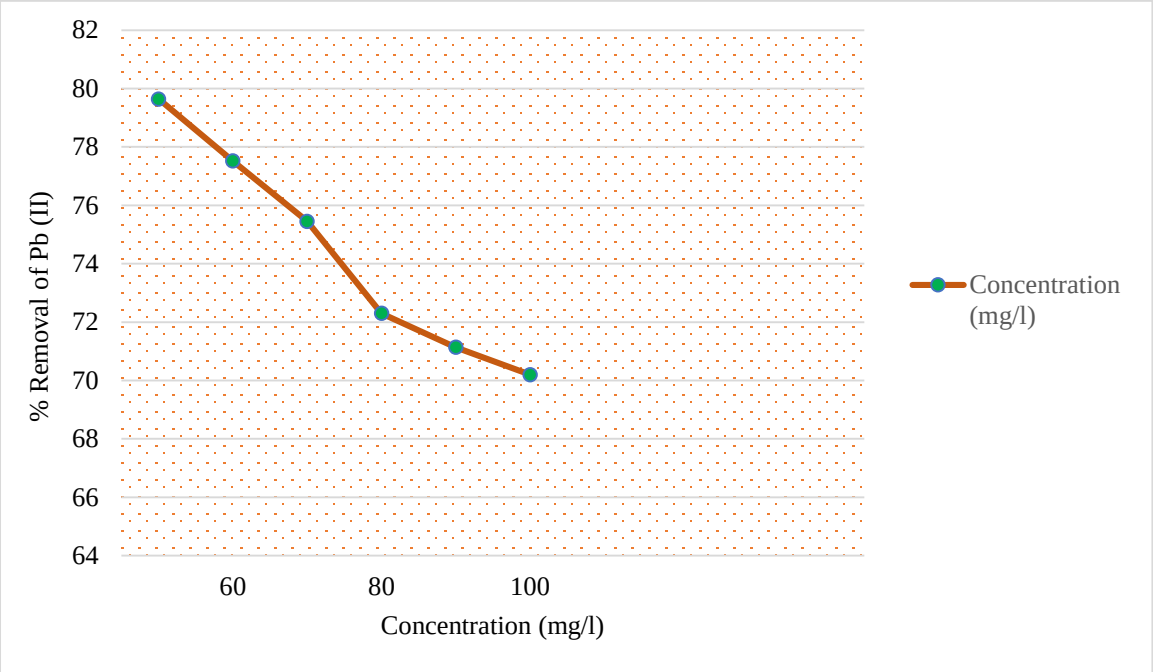

Figure 9: Adsorption of lead (II) ions as a function of ion concentration

4.1.5 Adsorption Isotherm modeling for Pb (II) ions

The relationship between the adsorbed quantity of metal ions and their equilibrium concentration in the solution could be graphically shown by referring to adsorption isotherms. Table 1 details the methods used to evaluate the experimental data from this investigation, which included three isotherm models—Langmuir being the most prominent—to investigate the RM-mediated adsorption of Pb (II). Metal ion distribution between solid and liquid phases is described by these models, which include Freundlich and Langmuir. Using these, we were able to learn about the adsorption process and find out how much ion concentration (from 50 to 100 mg/l) could be adsorbed.

Table 1.Adsorption characteristics of lead (II) ions on the adsorbents as determined using the Langmuir isotherm

Isotherm Model	Red Mud
Langmuir Isotherm parameters	
$q_m(mg/g)$	16.39
$K_L(l/mg)$	0.0525
R_L	0.275
R^2	0.99

The Langmuir isotherm explains not only how metal ions are distributed throughout the adsorbent and adsorbate, but also how adsorption on homogenous adsorption sites happens in a monolayer. The line that was drawn when Ce was plotted against Ce/qe allowed us to find the constants qm and kL by analyzing the slope and intercept, respectively. With a maximum value of 16.39 mg/g, RM achieved the largest adsorption capacity (qm) per gram, as reported in Table 2 of the Langmuir isotherm. The RM R^2 score of 0.99 indicates that the isotherm framework agreed well with the observed data.

The Langmuir constant K_L, which reflects the energy of adsorption (l/mg), was determined to be 0.0525 l/mg. This suggests that RM exhibited a strong affinity for the adsorbate. The separation factor RL is an additional critical parameter of the Langmuir isotherm. Good adsorption is indicated by a

value between 0 and 1, while an unfavorable process is shown by RL> 1. According to the results, the RL value for RM was 0.275, suggesting that the two adsorbents had a good affinity for Pb (II) ions.

Table 2.Adsorption properties of Pb (II) ions on the adsorbents as described by the Freundlich isotherm

Isotherm Model	Red Mud
Freundlich Isotherm parameters	
$K_F(l/g)$	1.753
N	1.9
R^2	0.988

Adsorption on heterogeneous surfaces is suggested by the Freundlich isotherm, which is used to evaluate the adsorbent's adsorption capability against the adsorbate.A linear connection was found by plotting log Cevs log qe; the intercept and slope were used to compute the coefficients kF and n, respectively. A kF value of 1.753 was found for RM adsorbents. If the calculated n value is between 1 and 10, then the adsorption conditions are favorable.As shown in Table 3, the n values for RM were found to be 1.9, confirming the favorable adsorption of Pb (II). The correlation coefficient (R2) values for both adsorbents indicated a good fit of experimental data with the isotherm models.

4.2Chromium (VI) Ion Removal

4.2.1 Effect of pH

The ideal pH for Cr (VI) adsorption onto the adsorbents was determined by exploring pH ranges between 1 and 10. The pH was adjusted within this range by dropwise addition of hydrochloric acid and sodium hydroxide. 0.5 grams of RM adsorbents were used to adsorb Cr (VI) ions in a 100 ml volume. Figure 10 illustrates that the maximum adsorption occurred at pH 6 for RM. Between pH 3-7, a gradual increase in adsorption occurred, with RM achieving a maximum removal efficiency of 78.21% for Cr (VI) ions. At pH levels above 8, chromium hydroxide likely formed due to an excess of OH- ions, leading to precipitation and a subsequent decrease in metal ion uptake.

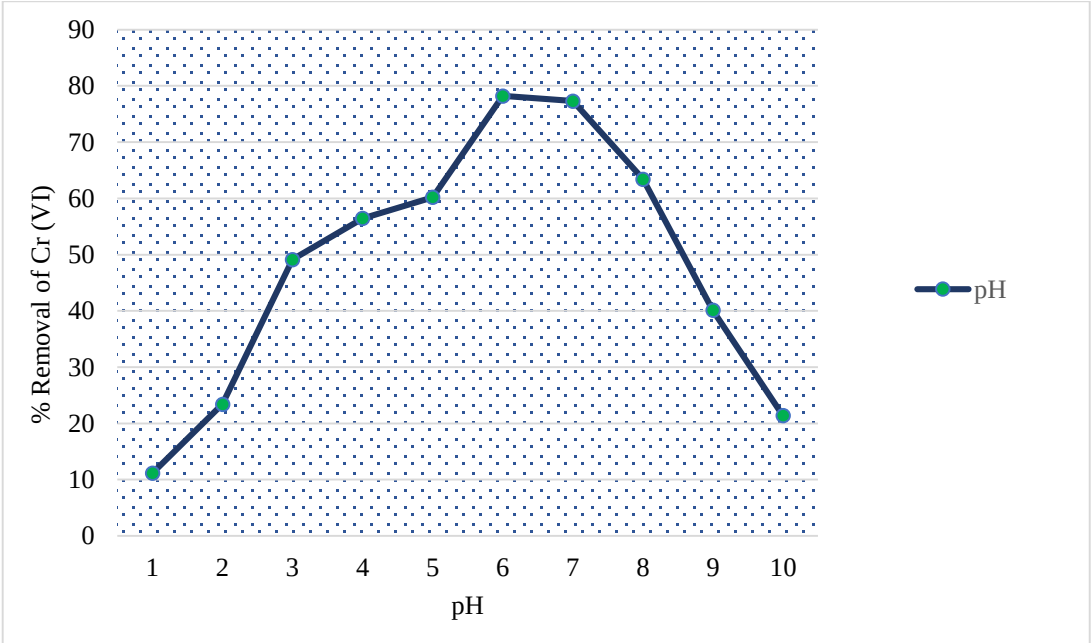

Figure 10: Cr (VI) ion absorption as a function of pH

4.2.2 Effect of Absorbent Dosage

To effectively remove Cr (VI), it is essential to optimise the adsorbent dose. The optimal pH was maintained when metal ion solutions containing adsorbents of varying weights (0.1–0.8 g) were combined with these solutions at a concentration of 50 mg/l. After agitation, filtrates were analyzed, revealing that the highest adsorption occurred at 0.6 g of RM adsorbent. Figure 11 illustrates that increasing the quantity of adsorbent enhanced surface site availability, consequently increasing the removal percentage. However, additional adsorbent led to interactions that slightly reduced the removal percentage.After applying RM, the greatest percentage of Cr (VI) ions that could be removed was 76.26%.

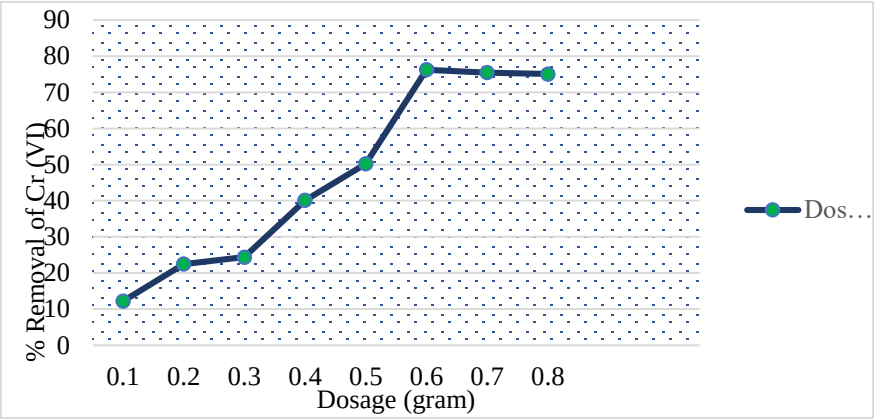

Figure 11: Ions of Cr (VI) adsorption as a function of adsorbent dose

4.2.3 Effect of contact time

The adsorption of Cr (VI) ions was investigated by varying the contact time between 15 and 105 minutes, while keeping the adsorbent dosage and pH at optimal levels. The study determined that a contact time of 60 minutes was most effective for RM, achieving a 74.85% removal of Cr (VI) ions. Figure 12 shows that RM reached a maximum uptake of 37.43 mg/L of Cr (VI) ions.Initially, there was a rapid uptake of metal ions by the adsorbent. However, over time, the adsorption rate slowed down as the available adsorbent surfaces became saturated with metal ions. This eventually led to the attainment of equilibrium after the optimized time period.

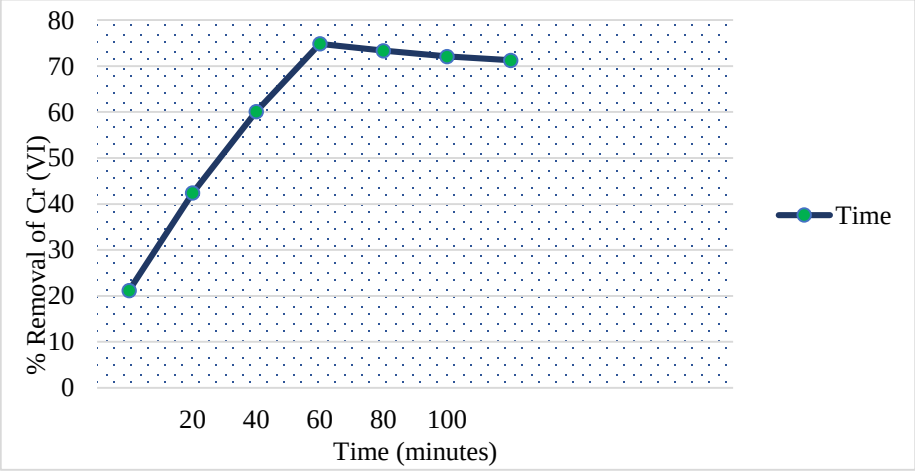

Figure 12: The adsorption of Cr (VI) ions in relation to contact time

4.2.4 Effect of concentration time of Cr (VI) ions

Figure 13 presents the findings from a study on how the initial concentration of Cr (VI) ions influenced the effectiveness of their removal. While optimizing the pH, dosage, and contact duration, the concentration was adjusted between 50 and 100 mg/l. Figure 13 clearly shows that the adsorbents achieved their maximum % removal and absorption of Cr (VI) ions at an initial concentration of 50 mg/l. At lower ion concentrations, there are more active sites on the adsorbent, which allows for easier ion binding.As the ion concentration increased with constant adsorbent quantities, the adsorbent surface sites approached saturation, resulting in decreased adsorption efficiency. The highest rate of Cr (VI) elimination that RM was able to accomplish was 75.01%. Under these circumstances, RM was able to reach its maximal absorption of Cr (VI) ions at 37.55 mg/l.

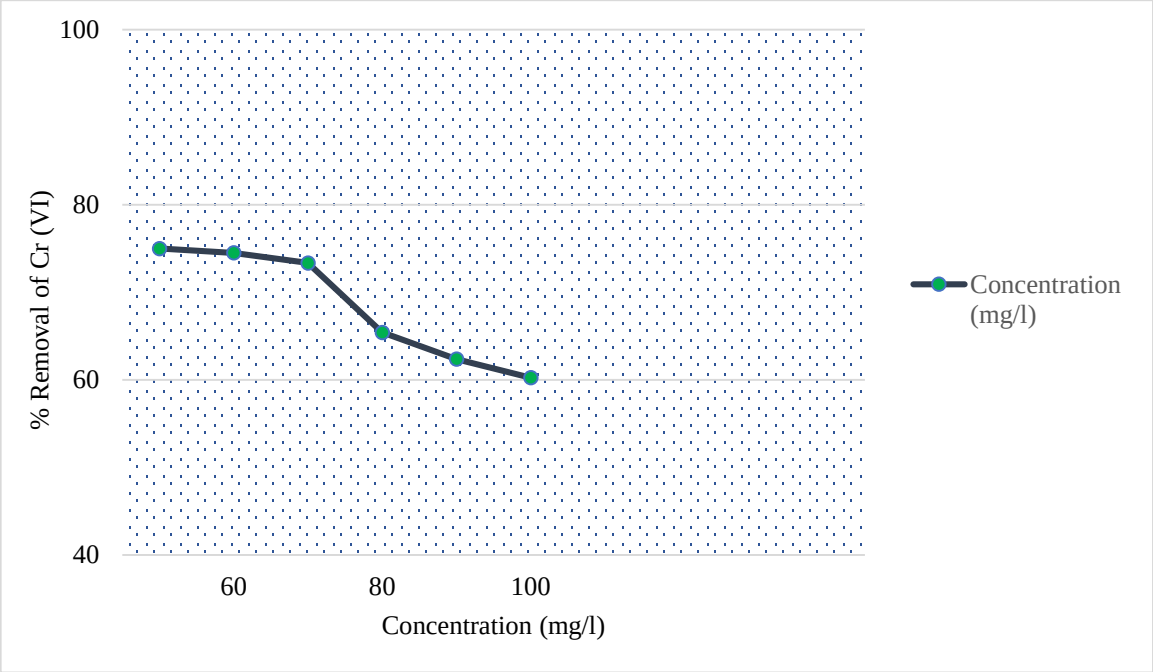

Figure 13: Adsorption of Cr (VI) ions in relation to ion concentration

4.2.5 Adsorption Isotherm modeling for Cr (VI) ions

The adsorption equilibrium of Cr (VI) metal ions on the adsorbents was analyzed using isotherm models, namely Langmuir and Freundlich, among others, to evaluate the effectiveness of the adsorbents.

Table 3.Adsorption characteristics for Cr (VI) ions on the adsorbents as determined using Langmuir isotherms

Isotherm Model	Red Mud
Langmuir Isotherm parameters	
$Q_m(mg/g)$	13.33
$K_L(l/mg)$	0.0776
R_L	0.204
R^2	0.994

The Langmuir isotherm approach presupposes that the adsorbent surface has a single layer of adsorption. The parameters Q_m(maximum adsorption capacity per gram of adsorbent) and kL (Langley constant linked to adsorption energy in l/mg) were calculated from a straight line plotted against C_e/q_e. Table 3 shows that the greatest adsorption capacity qm for RM was 13.33 mg/g, as revealed by the Langmuir isotherm. For RM, the computed kL values were 0.0776 l/mg, suggesting that the adsorbents bind strongly to the Cr (VI) ions.This empirical work further confirmed the favorable adsorption of Cr (VI) ions, since the separation factor RL, which ranges from 0 to 1, was determined to be 0.20 for RM. Furthermore, the empirical findings and the Langmuir isotherm models showed good agreement with an R^2 value of 0.994 for the adsorption of Cr (VI) ions onto RM.

Table 4.Cr (VI) ion adsorption Freundlich isotherm parameters on the adsorbents

Isotherm Model	**Red Mud**
Freundlich Isotherm parameters	
$K_F(l/g)$	2.094
n	2.21
R^2	0.978

The Freundlich isotherm assumes a heterogeneous adsorption surface. By plotting the graph of log Ce versus log q_e, the Freundlich adsorption capacity (K_F) and the Freundlich isotherm constant (n) were determined. The K_F value was derived from the intercept, while n was calculated from the slope. The obtained n value, falling between 1 and 10, indicated favorable adsorption conditions. According to Table 4, the n values for Cr (VI) adsorption on RM were respectively 2.2, confirming favorable adsorption of Cr (VI) ions.The adsorption capacity (K_F) obtained was 2.09 for RM, indicating effective adsorption capacities for both adsorbents. Furthermore, a high R^2 of 0.978 for the adsorption of Cr (VI) ions onto RM demonstrated excellent agreement between experimental values and the Freundlich isotherm model.

5. CONCLUSION AND FUTURE SCOPE

The study on the adsorption behavior of industrial waste using RM as an absorbent has provided valuable insights into its efficacy in removing contaminants from wastewater. The experimental findings reveal that RM exhibits significant adsorption capacities, achieving a maximum q_m of 13.33 mg/g according to Langmuir isotherms, and an n value of 2.21 from Freundlich isotherms, highlighting its versatility in different adsorption scenarios. Optimization of parameters such as pH, adsorbent dosage, and contact time has shown to enhance its performance in removing contaminants effectively. The research underscores RM potential as a viable and cost-effective adsorbent for treating industrial wastewater, offering promising implications for environmental sustainability and remediation efforts. Further studies could explore its application in larger-scale industrial settings and assess its long-term effectiveness and economic viability.

REFERENCES

1. Water, U. N. Water and Jobs. The United Nations World Water Development Report 2016 https://www.unwater.org/publications/world-water-development-report2016/ (2016).
2. Mutamim, N. S. et al. Membrane bioreactor: Applications and limitations in treating high strength industrial wastewater. Chem. Eng. J. 225, 109–119 (2013).
3. Lin, H. et al. Membrane bioreactors for industrial wastewater treatment: a critical review. Crit. Rev. Environ. Sci. Technol. 42, 677–740 (2012).
4. Hai, F. I., Yamamoto, K. & Lee, C.-H. Membrane Biological Reactors Theory, Modeling, Design, Management and Applications to Wastewater Reuse. (IWA Publishing, 2013).

5. Smythe, G., Matelli, G., Bradford, M. & Rocha, C. Biological treatment of salty wastewater. Environ. Prog. 16, 179–183 (1997).
6. UN. Wastewater management a UN-water analytical brief Analytical Brief. UN Water (2014).
7. UNESCO. Water in a changing world. The United Nations World Water Development Report 3. United Nations Educational, scientific and Cultural Organization (2009).
8. Ferella, F., De Michelis, I., Zerbini, C. &Vegliò, F. Advanced treatment of industrial wastewater by membrane filtration and ozonization. Desalination 313, 1–11 (2013).
9. Ahmed, Menatalla, Musthafa O. Mavukkandy, AdewaleGiwa, Maria Elektorowicz, EvinaKatsou, OlfaKhelifi, Vincenzo Naddeo, and Shadi W. Hasan. "Recent developments in hazardous pollutants removal from wastewater and water reuse within a circular economy." NPJ Clean Water 5, no. 1 (2022): 1-25.
10. Fawell J, Ong CN. Emerging contaminants and the implications for drinking water. International Journal of Water Resources Development. 2012;28:247-263.
11. Ismail, Wan Norfazilah Wan, and SitiUmairahMokhtar. "Various methods for removal, treatment, and detection of emerging water contaminants." Emerging contaminants (2020).
12. Falconer IR, Chapman HF, Moore MR, Ranmuthugala G. Endocrine-disrupting compounds: A review of their challenge to sustainable and safe water supply and water reuse. Environmental Toxicology. 2006;21:181-191.
13. Petrovic M. Analysis and removal of emerging contaminants in wastewater and drinking water. TrAC Trends in Analytical Chemistry. 2003;22:685-696.
14. Huang Q , Bu Q , Zhong W, Shi K, Cao Z, Yu G. Derivation of aquatic predicted no-effect concentration (PNEC) for ibuprofen and sulfamethoxazole based on various toxicity endpoints and the associated risks. Chemosphere. 2018;193:223-229.
15. Oetjen K, Giddings CGS, McLaughlin M, Nell M, Blotevogel J, Helbling DE, et al. Emerging analytical methods for the characterization and quantification of organic contaminants in flowback and produced water. Trends in Environmental Analytical Chemistry. 2017;15:12-23.
16. O. Oladoye, M. O. Bamigboye, O. D. Ogunbiyi, M. T. Akano,Groundwater Sustainable Dev. 2022, 19, 100844.
17. S. F. Azha, M. Shahadat, S. Ismail, S. W. Ali, S. Z. Ahammad,J. Taiwan Inst. Chem. Eng. 2021, 120, 178–206.
18. E. M. Nigri, A. L. A. Santos, S. D. F. Rocha, J. Water ProcessEng. 2020, 37, 10144.
19. X. Pang, S. Lotfi, F. Dison, D. GuilhermeLuiz, G. Jordana,B. Abdullah, B. Hafedh, B. L. Abdelmottaleb, A. Bonilla-Petriciolet, L. Zichao, Chem. Eng. J. 2019, 378, 122101.
20. G. Crini, E. Lichtfouse, L. D. Wilson, N. Morin-Crini, inGreen Adsorbents for Pollutant Removal (Eds: G. Crini,E. Lichtfouse), Springer, Berlin 2018, 23–71.
21. Somashekara, Divyashree, and LavanyaMulky. "Sequestration of contaminants from wastewater: a review of adsorption processes." *ChemBioEng Reviews* 10, no. 4 (2023): 491-509.
22. Bošković, Ivana, SlađanaGoranović, Mira Vukčević, LjiljanaKljajević, SnežanaNenadović, MarijaIvanović, and JelenaGulicovski. "Red mud-fly ash-based geopolymers as an eco-friendly material for immobilization of toxic pollutants (Pb and Cu) from wastewater." *Science of Sintering* 00 (2024): 24-24.
23. Le, Quynh Hoang, KamelSmida, Zahra Abdelmalek, and IskanderTlili. "Removal of heavy metals by polymers from wastewater in the industry: A molecular dynamics approach." *Engineering Analysis with Boundary Elements* 155 (2023): 1035-1042.

24. Chyad, TasnimFahim, RawaaFahimChyad Al-Hamadani, ZamanAgeelHammood, and GhasaqAbd Ali. "Removal of Zinc (II) ions from industrial wastewater by adsorption on to activated carbon produced from pine cone." *Materials Today: Proceedings* 80 (2023): 2706-2711.

25. An, Dongdong, Yu Sun, Yan-Ling Yang, Xiao-Lei Shi, Hua-Jun Chen, Li Zhang, GuoquanSuo et al. "A strategy-purifying wastewater with waste materials: Zn2+ modified waste red mud as recoverable adsorbents with an enhanced removal capacity of congo red." *Journal of Colloid and Interface Science* 645 (2023): 694-704.

26. Carvalheiras, João, Rui M. Novais, and João A. Labrincha. "Metakaolin/red mud-derived geopolymer monoliths: Novel bulk-type sorbents for lead removal from wastewaters." *Applied Clay Science* 232 (2023): 106770.

27. Xu, Wenbin, Hailang Yang, Qiming Mao, Lin Luo, and Ying Deng. "Removal of heavy metals from acid mine drainage by red mud–based geopolymer pervious concrete: Batch and long–term column studies." *Polymers* 14, no. 24 (2022): 5355.

28. Lyu, Fei, SulinNiu, Li Wang, Runqing Liu, Wei Sun, and Dongdong He. "Efficient removal of Pb (II) ions from aqueous solution by modified red mud." *Journal of Hazardous Materials* 406 (2021): 124678.

29. Elboughdiri, Noureddine. "The use of natural zeolite to remove heavy metals Cu (II), Pb (II) and Cd (II), from industrial wastewater." *Cogent Engineering* 7, no. 1 (2020): 1782623.

30. Friedrich, W.; Knipping, P.; Laue, M. InterferenzerscheinungenBeiRöntgenstrahlen. *Ann. Phys.* **1913**, *346*, 971–988.

31. Authier, A. *Early Days of X-ray Crystallography*; Oxford University Press: Oxford, UK, 2013.

32. Singh, A.K. *Advanced X-ray Techniques in Research and Industry*; IOS Press: Amsterdam, The Netherlands, 2005; ISBN 1586035371.

33. Bragg, W.L.; Thomson, J.J. The Diffraction of Short Electromagnetic Waves by a Crystal. *Proc. Camb. Philos. Soc. Math. Phys. Sci.* **1914**, *17*, 43–57.

34. Surdu, Vasile-Adrian, and RomualdGyőrgy. "X-ray diffraction data analysis by machine learning methods—a review." *Applied Sciences* 13, no. 17 (2023): 9992.

35. Newell, T.; Tillotson, B.; Pearl, H.; Miller, A. Detection of electrical defects with SEMVision in semiconductor production mode manufacturing. In Proceedings of the 2016 27th Annual SEMI Advanced Semiconductor Manufacturing Conference, Saratoga Springs, NY, USA, 16–19 May 2016; pp. 151–156.

36. Jain, A.; Sheridan, J.G.; Levitov, F.; Aristov, V.; Yasharzade, S.; Nguyen, H. Inline SEM imaging of buried defects using novel electron detection system. In Proceedings of the 2018 29th Annual SEMI Advanced Semiconductor Manufacturing Conference (ASMC), Saratoga Springs, NY, USA, 30 April–3 May 2018; pp. 259–263.

37. López de la Rosa, Francisco, Roberto Sánchez-Reolid, José L. Gómez-Sirvent, Rafael Morales, and Antonio Fernández-Caballero. "A review on machine and deep learning for semiconductor defect classification in scanning electron microscope images." *Applied Sciences* 11, no. 20 (2021): 9508.

38. J. Murphy and J. P. Riley, "A modified single solution method for the determination of phosphate in natural waters," AnalyticaChimicaActa, vol. 27, pp. 31–36, 1962.

39. State Environmental Protection Adminstraion, Monitoring and Analysis Method of Water and Wastwater, vol. 7, Environmental Science Press, Beijing, China, 2002.

40. S. Dursun, D. Guclu, and M. Bas, “Phosphate removal by using activated red mud from SeydisehirAluminium Factory in Turkey,” Journal of International Environmental Application & Science, vol. 1, no. 3-4, pp. 98–106, 2006.
41. Abbasi, Somayeh, RaufForoutan, HosseinEsmaeili, and FeridunEsmaeilzadeh. "Preparation of activated carbon from worn tires for removal of Cu (II), Ni (II) and Co (II) ions from synthetic wastewater." *Desalin. Water Treat* 141 (2019): 269-278.
42. Abas, S. N. A., M. H. S. Ismail, M. L. Kamal, and S. Izhar. "Adsorption process of heavy metals by low-cost adsorbent: a review. World ApplSci J 28: 1518–1530." (2013).
43. Chakraborty, Rupa, AnupamaAsthana, Ajaya Kumar Singh, Bhawana Jain, and Abu Bin Hasan Susan. "Adsorption of heavy metal ions by various low-cost adsorbents: a review." *International Journal of Environmental Analytical Chemistry* 102, no. 2 (2022): 342-379.